

G1 Phase Regulation, Area-Specific Cell Cycle Control, and Cytoarchitectonics in the Primate Cortex

Agnès Lukaszewicz,^{1,4} Pierre Savatier,^{1,2}
Véronique Cortay,^{1,2} Pascale Giroud,¹
Cyril Huissoud,^{1,2,3} Michel Berland,^{1,3}
Henry Kennedy,¹ and Colette Dehay^{1,2,*}

¹Department of Stem Cell and Cortical Development
INSERM U371

Cerveau et Vision, IFR19
Université Claude Bernard Lyon I
18 avenue du Doyen Lépine
69500 Bron

France
²PrimaStem
18 avenue du Doyen Lépine
69500 Bron

France
³Hôpital Lyon Sud
Chemin du Grand Revoyet
69495 Pierre-Bénite
France

Summary

We have investigated the cell cycle-related mechanisms that lead to the emergence of primate areas 17 and 18. These areas are characterized by striking differences in cytoarchitectonics and neuron number. We show *in vivo* that (1) area 17 precursors of supragranular neurons exhibit a shorter cell cycle duration, a reduced G1 phase, and a higher rate of cell cycle reentry than area 18 precursors; (2) area 17 and area 18 precursors show contrasting and specific levels of expression of cyclin E (high in area 17, low in area 18) and p27^{Kip1} (low in area 17, high in area 18); (3) *ex vivo* up- and downmodulation of cyclin E and p27^{Kip1} show that both regulators influence cell cycle kinetics by modifying rates of cell cycle progression and cell cycle reentry; (4) modeling the areal differences in cell cycle parameters suggests that they contribute to areal differences in numbers of precursors and neuron production.

Introduction

Primate corticogenesis shares key features with that in the rodent, including peripheral control of arealization and early patterning of the germinal zone and cortical plate (Kennedy and Dehay, 1993; Rakic, 1974; Sestan et al., 2001). However, a number of recent studies have revealed the existence of primate-specific developmental features (Letinic et al., 2002; Meyer et al., 2000; Smart et al., 2002), indicating that the monkey is of special importance for understanding human cortical development.

*Correspondence: dehay@lyon.inserm.fr

⁴Present address: California Institute of Technology, Division of Biology, 216-76, 1200 East California Boulevard, Pasadena, California 91125.

Areal differences in cytoarchitectonics and neuron number are a general feature of the cortex that has been documented in rodents, carnivores, and primate (Beaulieu and Colonnier, 1989; Garey et al., 1985; Rockel et al., 1980; Skoglund et al., 1996). In the primate, areas 17 and 18 of the visual cortex have strikingly different numbers of neurons in granular and supragranular layers (Rockel et al., 1980). We have used this model system, in which the germinal zones of presumptive areas 17 and 18 can be unambiguously identified during early stages of corticogenesis, to investigate the contribution of the cell cycle regulation of cortical precursors in areal specification.

In the primate, there are regional differences in tritiated thymidine uptake by the precursors in the germinal zones producing areas 17 and 18 during the generation of supragranular layer neurons, suggesting possible regional variations of cell cycle dynamics (Dehay et al., 1993). Patterning and growth are linked via cell cycle control. Regional differences in the proliferative program can have far-reaching consequences for histogenesis of cortical areas. Firstly, there is evidence of molecular coordination of cell cycle components and factors promoting neuronal determination/differentiation process (Ohnuma and Harris, 2003; Ohnuma et al., 2001), suggesting that cell cycle regulation could impact on cell fate in cortical precursors. Secondly, because the pyramidal phenotype is specified by signals acting on cycling precursors (McConnell and Kaznowski, 1991; Polleux et al., 2001), variations in rates of proliferation at a given stage of histogenesis will lead to variations in the number of a particular phenotype being produced and therefore suggest a mechanism that can effectively link areal and laminar fate.

The interrelationship of areal and laminar specification requires that the specification of cells to a regional fate is coupled to the regulated expansion of the precursor pool so as to generate the appropriate numbers of neurons in each of the layers that make up the cytoarchitecturally distinct areas. The differences in tritiated thymidine uptake in the germinal zone generating areas 17 and 18 could hypothetically reflect modulation of neuron production via the regulation of the size of the precursor pool (Dehay et al., 1993).

To investigate this issue, we have examined area-specific cell cycle kinetics and its molecular correlate in precursors of areas 17 and 18. The coordinated regulation of two cardinal parameters of the cell cycle is essential to regulate the size of the precursor pool (Rakic, 1995): (1) the balance between reentry or exit of the cell cycle and (2) rate of cell cycle progression.

These two parameters are controlled by cell cycle regulators, cyclins, cyclin-dependent kinases (Cdk), and Cdk inhibitors (CKI). Of prime importance is cyclin E, which binds to and activates Cdk2, thereby promoting entry in S phase in a rate-limiting manner (Resnitzky et al., 1994). Contrarily, the CKI p27^{Kip1} is chiefly a negative regulator of the G1 to S phase transition, which binds to cyclin E:Cdk2 and inhibits its activity (Polyak et al., 1994; Sherr and Roberts, 1999). p27^{Kip1}^{-/-} mice

have enlarged and hypercellular brain structures as well as general hyperplasia reflecting impaired withdrawal from the cell cycle in response to antimitogenic signals (Kiyokawa et al., 1996). Hence, cyclin E and p27kip1 play antagonistic roles in the control of Cdk2 activity and promotion of S phase entry, and here we have explored the involvement of these genes in the regulation of the cell cycle in the germinal zones of areas 17 and 18.

The present study demonstrates important differences in both the duration of the G1 phase of the cell cycle and mode of division of precursors of areas 17 and 18. Can the observed shorter cell cycle of area 17 precursors lead to increased neuron production despite their lower rate of cell cycle exit? To investigate this issue, we modeled the observed differences in cell cycle parameters, and this shows that areal differences in these parameters lead to significantly higher rates of neuron production in area 17 compared to area 18.

Ex vivo experimental up- and downmodulation of cyclin E and p27^{kip1} show that these two regulators of cell cycle progression—acting via the control of the G1/S transition—are involved in the observed areal variation in cell cycle kinetics.

The present study suggests that G1 phase regulation could have far-reaching consequences for cortical development in the building of distinct cortical areas. Interestingly, a number of neuronal determination and proliferation-promoting signals exert their influence through G1 cell cycle components (Baek et al., 2003; Kioussi et al., 2002; Oliver et al., 2003).

Results

We have investigated corticogenesis specifically in relationship to cytoarchitecture. We have addressed five main issues using in vivo and ex vivo approaches: (1) the identity of the precursor pool of supragranular layers of areas 17 and 18; (2) the cell cycle parameters of the precursors of the supragranular layers of areas 17 and 18; (3) the differential expression in areas 17 and 18 of cell cycle regulators; (4) up- and downmodulation of the G1/S transition regulators on organotypic slices to confirm their role in modifying cell cycle parameters; (5) modeling of the observed areal differences in cell cycle parameters.

Germinal Origin of Supragranular Layer Neurons

The germinal zones of the monkey embryonic cortex are characterized by the emergence of a precursor pool: the OSVZ (outer subventricular zone), which is unique to the primate. The OSVZ individualizes from the SVZ circa E62 (Smart et al., 2002). During the production of supragranular layers, the SVZ is subdivided into an inner SVZ (ISVZ) and an outer SVZ (OSVZ) as revealed by the cytological organization of the precursors and the location of abventricular mitosis (Figure 1) (Smart et al., 2002).

So as to identify the pool of precursors that generate the supragranular layers, we have carried out a series of 3H-thymidine injections at different development stages coupled with variable survival times. A 3H-thymidine pulse at E64 followed by a short survival time (3 hr) shows that, during the production of infragranular

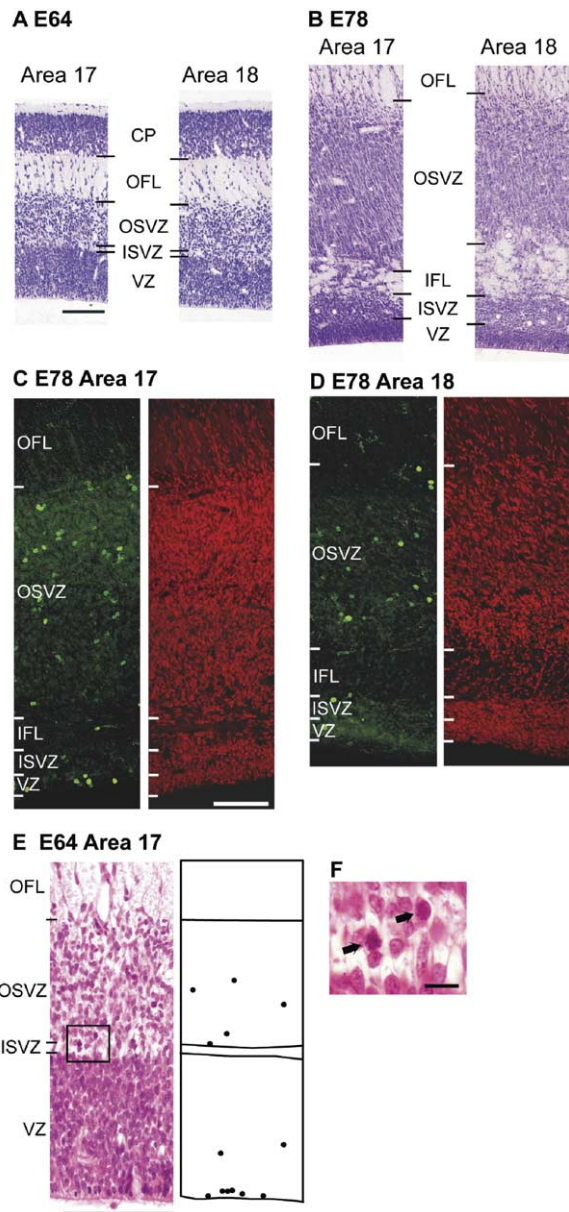


Figure 1. Compartmentation of the Primate Germinal Zones

(A) Nissl-stained parasagittal sections (5 μm thick) cutting through area 17 and area 18 germinal zones at E64. (B) Nissl-stained parasagittal sections (5 μm thick) cutting through area 17 and area 18 germinal zones at E78. (C) H3 immunolabeling showing the location of mitosis in area 17 germinal zones at E78. Abventricular mitosis is observed in the ISVZ and OSVZ. Adjacent microphotograph shows fluorescent nuclei staining with propidium iodide. (D) H3 immunolabeling showing the location of mitosis in area 18 germinal zones at E78. Adjacent microphotograph shows fluorescent nuclei staining with propidium iodide. (E) Eosin-hematoxylin-stained section (5 μm thick) of the germinal zones of area 17 at E64. Mitotic figures are observed in the ISVZ and OSVZ as indicated on the chart. (F) High-power microphotograph showing abventricular mitosis from the insert in (E). CP, cortical plate; IFL, inner fiber layer; ISVZ, inner subventricular zone; MZ, marginal zone; OFL, outer fiber layer; OSVZ, outer subventricular zone; SP, subplate; VZ, ventricular zone; WM, white matter. Scale bars in (A)–(E), 100 μm ; scale bar in (F), 10 μm .

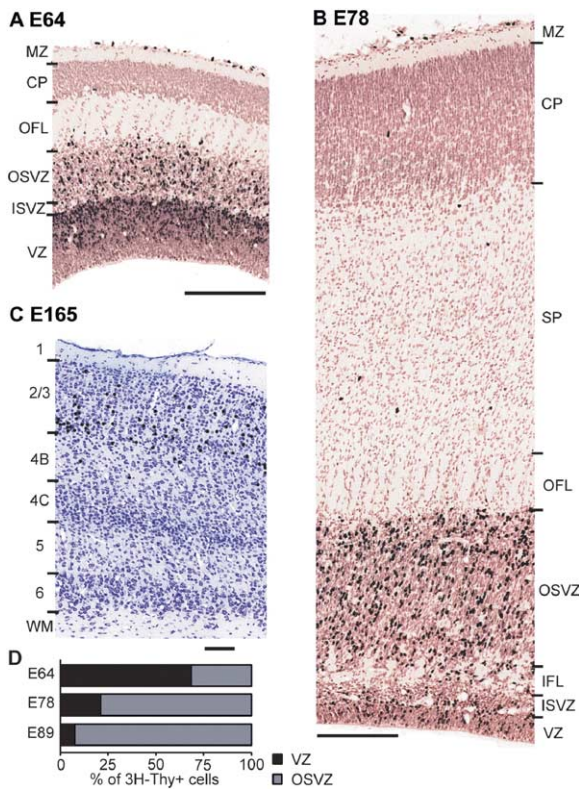


Figure 2. Germinal Origin of Cortical Neurons (A) Area 17, E64 3H-thymidine pulse, 3 hr survival. (B) Area 17, E78 3H-thymidine pulse, 1 hr survival. (C) Area 17, E78 3H-thymidine pulse, 87 day survival. (D) Distribution of labeled precursors in OSVZ and VZ at E64, E78, and E89. Abbreviations as in Figure 1. Scale bars, 100 μ m.

layers (Rakic, 1974), 70% of labeled S phase neuroblasts are located in the ventricular zone (VZ) (Figures 2A and 2D). In contrast, short survival periods (1 hr) following E78 and E89 pulses reveal that 80%–90% of labeled precursors are located in the OSVZ (Figures 2B and 2D), which has reached its maximum extent at these ages (Smart et al., 2002). Examination in the newborn cortex of the autoradiographic labeling following a 3H-thymidine pulse at E78 shows large numbers of labeled neurons in layers 2/3 (Figure 2C). These results show that the OSVZ is the major site of production of neurons destined for the supragranular layers.

Characterization of Cell Cycle Kinetics of Areas 17 and 18 In Vivo

First, we developed a stable in vitro assay system in which cycling precursors (corresponding to the growth fraction [GF]) are reliably identified by PCNA expression, and postmitotic neurons are identified by MAP2 expression (Dehay et al., 2001; Lukaszewicz et al., 2002) (Figure 3A). At E78, compared to area 18, area 17 dissociated precursors show higher rates of proliferation, as indicated by a more rapid increase in cell density (CD) (Figure 3B). Using BrdU as an S phase marker, we further characterized the proliferation rates by computing the labeling index (LI), i.e., the percentage of

PCNA-positive cells that have incorporated BrdU after an 8 hr exposure. The LI indicates the proportions of precursors in S phase at the time of the BrdU pulse and therefore reflects the relative duration of S phase (T_s) with respect to the total duration of the cell cycle (T_c). LI values did not differ between the two sets of precursors at E62 (Figure 3C). However, at E78, area 17 precursors showed significantly higher LI values than area 18, indicating differences in cell cycle kinetics (Figure 3D).

Second, we investigated the in vivo duration of the individual phases of the cell cycle in precursors of the OSVZ in each area by combining S phase cumulative labeling technique (Nowakowski et al., 1989) and computation of the percentage of labeled mitosis (PLM) (Quastler and Sherman, 1959). The cumulative S phase labeling procedure makes it possible to calculate T_c , T_s , and the combined duration of G1, G2, and M phases ($T_{g1} + g2/m$) (Figure 3E). The proportion of cells labeled by 3H-thymidine (LI) was monitored at two points within the estimated duration of T_c (Kornack and Rakic, 1998). The LI values have been corrected with the GF values measured in the OSVZ of area 17 and area 18 at E78 by means of PCNA immunostaining (see Experimental Procedures). The cumulative 3H-thymidine labeling performed at E78 shows that the two sets of precursors have identical T_s (9 hr) and significant differences in the duration of $T_{g1} + g2/m$ (area 17, 27 hr; area 18, 37 hr) (Figure 3F).

Following a pulse injection of 3H-thymidine, the time interval required for 100% labeling of mitotic figures corresponds to the passage through G2 and M (PLM method) (Figure 3G). This returns identical values for $T_{g2} + m$ of 8 hr for both area 17 and area 18 precursors (Figure 3H). Hence, T_c is 36 hr for area 17 precursors and 46 hr for area 18 precursors. This difference in cell cycle length is exclusively due to a 51% difference in T_{g1} (area 17, 19 hr; area 18, 29 hr). Computation of the percentage of mitotic figures in the OSVZ of presumptive area 17 and area 18 shows a significantly higher proportion of precursors in M phase in area 17, confirming a faster cell cycle progression in this area (Figure 3I).

Area-Specific Levels of Expression of Cell Cycle Regulators

Next, we have analyzed the molecular correlate of the area-specific regulation of T_{g1} in the OSVZ precursors. We focused our analysis on cyclin E and p27^{Kip1}. In vivo, both p27^{Kip1} and cyclin E are expressed by cortical precursors of the VZ and the OSVZ (Figures 4A and 4B). Whereas p27^{Kip1} is expressed at detectable levels in all precursors and postmitotic cells (Lukaszewicz et al., 2002; Mitsuhashi et al., 2001; Zindy et al., 1999; Zindy et al., 1997) (Figures 4A and 4B; and see the Supplemental Data available with this article online), cyclin E expression is restricted to the fraction of precursors that are in G1/S transition (Ekholm et al., 2001; Wimmel et al., 1994) (Figure 4C).

In our first approach, we investigated cyclin E mRNA levels in area 17 and area 18 germinal zones at E82. Transcriptional activation of cyclin E plays a significant role in the cell cycle-dependent regulation of cyclin E expression (Bartek and Lukas, 2001). Real-time PCR

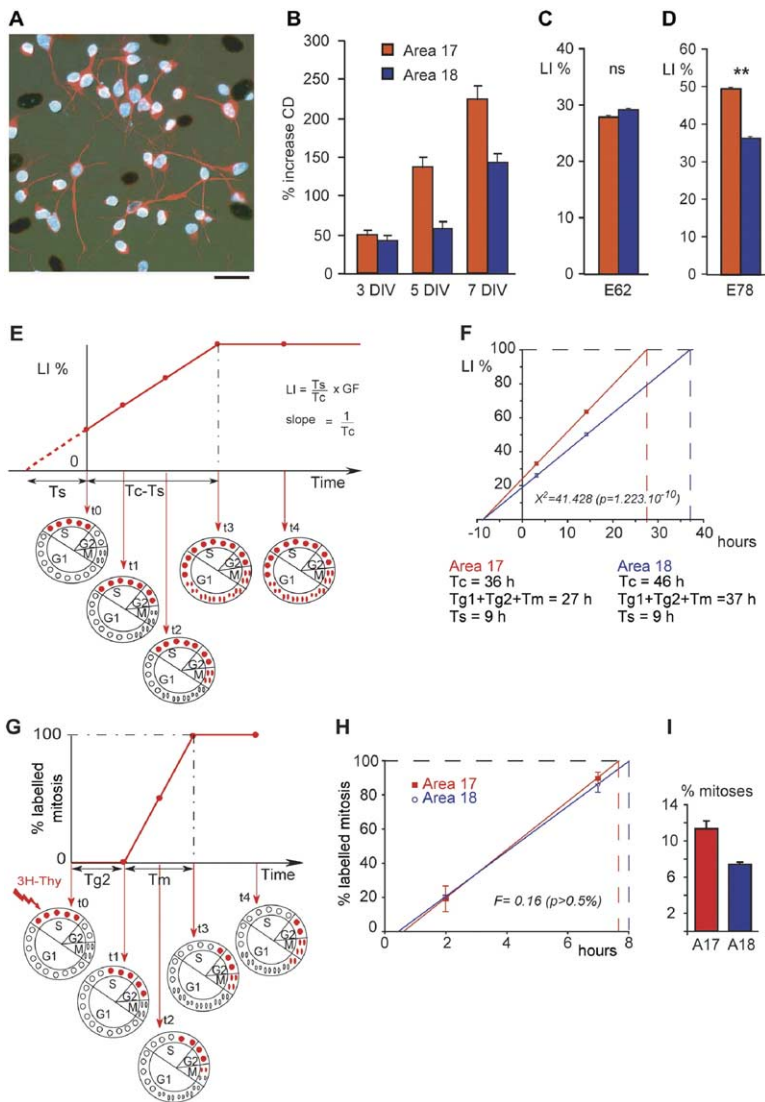


Figure 3. Cell Cycle Kinetics of Area 17 and 18 Precursors

(A) Microphotograph of E78 area 17 dissociated precursors. MAP2 (red) and PCNA (brown) immunolabeling at 4 DIV. Scale bar, 20 μ m.

(B–D) In vitro values. (B) Cell density (CD) values at E78. (C) LI values at E62 after 3 DIV; (D) LI values at E78 after 3 DIV. Values are \pm SEM. Statistical significance was assessed with Student's t test.

(E) Cartoon illustrating principles of 3H-thymidine cumulative labeling. This technique is based on a continuous 3H-thymidine exposure that leads to the incorporation of 3H-thymidine by successive cohorts of cycling cells progressing through S phase. The projection of the LI = 100% on the x axis gives Tc – Ts. Ts is given by the projection of LI = 0 on the x axis.

(F) 3H-thymidine cumulative labeling at E78 in vivo. Logistic regression combined with a χ^2 analysis shows that the two slopes are significantly different.

(G) Cartoon showing principles of PLM (percentage of labeled mitotic figures). This procedure, based on a brief exposure of cells to 3H-thymidine, measures the time required for cells in S phase to enter M phase and therefore returns Tg2/m.

(H) PLM values at E78. Statistical analysis (F test) shows that the slopes are identical.

(I) Percentage of mitosis in area 17 and area 18 OSVZ at E78. Values are \pm SEM.

analysis shows increased expression of cyclin E mRNA in area 17 germinal zones compared to area 18 (Figure 4D).

As the abundance of p27^{Kip1}—and also of cyclin E—is largely regulated by posttranslational mechanisms, in particular by proteolysis mediated by the ubiquitin-proteasome pathway (Nakayama et al., 2001), we therefore investigated p27^{Kip1} and cyclin E protein levels using confocal quantification of immunofluorescent labeling (Durand et al., 1997; Lukaszewicz et al., 2002; Tokumoto et al., 2002). Confocal quantification of immunofluorescent labeling against cyclin E over the full-width of the OSVZ in presumptive areas 17 and 18 shows significantly higher levels of tissular expression in area 17 compared to area 18 (Figure 4E). p27^{Kip1} in the OSVZ shows a contrasting expression pattern (Figure 4F).

However, because expression of p27^{Kip1} is upregulated in postmitotic cells (Lukaszewicz et al., 2002), areal differences in p27^{Kip1} expression at the tissue level could reflect regional variations in the proportions of precursors and postmitotic cells in the OSVZ rather than variations in cell cycle regulatory gene activity

within the cycling precursor pool. Further, cyclin E tissular expression could also be influenced by areal differences in the proportion of precursors in late G1 and in G1/S transition (cf. above). In order to pin down areal differences in the regulatory mechanisms that directly control cell cycle progression, it is therefore necessary to monitor the levels of gene expression at the single cell level within the cycling precursor pool. Confocal microscopy quantification of the levels of expression of cyclin E shows that individual precursors exhibit significantly higher levels of cyclin E expression in area 17 compared to area 18 (Figure 4G).

So as to restrict p27^{Kip1} analysis to the cycling cells, we used dissociated cell cultures (see above) where PCNA expression makes it possible to reliably identify the cycling population of precursors (Figures 4H, 4I, and 3A). Quantification of fluorescent immunoreactivity against p27^{Kip1} restricted to the PCNA-positive precursors revealed significantly lower levels of p27^{Kip1} expression in area 17 precursors compared to area 18 precursors (Figure 4J).

The present results show that, at both the population

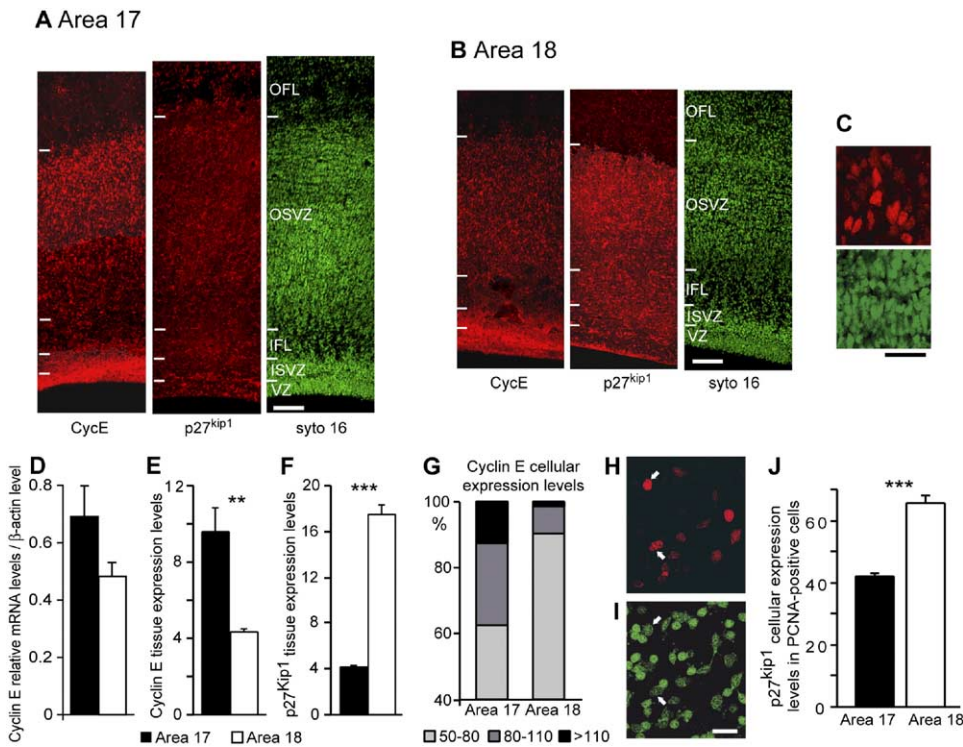


Figure 4. Tissue and Cellular Levels of Expression of Cyclin E and p27^{Kip1}

(A) Cyclin E, p27^{Kip1}, immunolabeling, and Syto16 counterstaining in area 17 germinal zones at E80. (B) Cyclin E, p27^{Kip1}, immunolabeling, and Syto16 counterstaining in area 18 germinal zones at E80. (C) (Upper panel) High magnification of cyclin E-positive precursors in the OSVZ, taken from (A); (lower panel) high magnification of OSVZ precursors counterstained with Syto16, showing that only a fraction of precursors express high levels of cyclin E. (D) Real-time PCR analysis of cyclin E mRNA levels at E82. (E) Tissue cyclin E expression levels (confocal quantification of cyclin E fluorescent immunolabeling corrected for cell density in the OSVZ). (F) Tissue p27^{Kip1} expression in area 17 and area 18 OSVZ (confocal quantification of p27^{Kip1} fluorescent immunolabeling corrected for cell density in the full-width of the germinal zone). (G) Proportions of cells with high, medium, and low cyclin E levels in area 17 and area 18 OSVZ. (H) Confocal image of PCNA nuclear immunostaining on dissociated precursors from area 17 after 2 DIV. (I) Confocal image of p27^{Kip1} immunolabeling (same field of view as [H]). (J) p27^{Kip1} cellular expression levels in PCNA-positive cells after 2 DIV. p27^{Kip1} levels of expression are significantly lower in area 17 precursors than in area 18 precursors. Scale bars, 100 μm in (A) and (B); 25 μm in (C); 50 μm in (H) and (I). For abbreviations, see Figure 1. Values are ±SEM.

and single cell levels, there are contrasting levels of expression of p27^{Kip1} and cyclin E in area 17 and area 18 precursors. These findings are in agreement with the higher rates of proliferation found in vivo in area 17.

Areal Differences in Frequency of Cell Cycle Reentry

We now need to address the frequency of cell cycle reentry, which also influences rates of neuron production in the cerebral cortex (Rakic, 1973; Rakic, 1995). The G1 phase is divided into pre- and postrestriction point (R) components, and markers of the postrestriction G1 phase can be used to identify daughter cells that are committed to cell cycle reentry (Ekholm et al., 2001; Zetterberg et al., 1995). Passage through R is a prerequisite for accumulation of cyclin E during a 2 hr period prior to entry in S phase, and cyclin E expression is limited to this narrow time window. Most of the protein is rapidly downregulated within 1 to 2 hr after entry into S phase (Ekholm et al., 2001). Hence, cyclin E expression constitutes a reliable marker of late G1 phase and therefore of precursor engagement in cell cycle re-

entry (Figure 5A). Analysis in the OSVZ shows that the proportion of precursors that are cyclin E positive and therefore engaged in cell cycle reentry is significantly higher in area 17 compared to area 18 (Figure 5B).

Role of p27^{Kip1} and Cyclin E in Modifying Rates of Cell Cycle Progression and Cell Cycle Reentry Revealed by Ex Vivo Upregulation and Downregulation Experiments

The above data suggest that differential expression levels of p27^{Kip1} and cyclin E in areas 17 and 18 OSVZ could be responsible for the area-specific differences in cell cycle parameters of supragranular precursors. To directly assess p27^{Kip1} and cyclin E gene function in areal differences in cell cycle kinetics, we performed upregulation (gain-of-function [GOF]) and downmodulation (loss-of-function [LOF]) experiments by using Lipofectamine 2000-mediated transfection on organotypic slices of E80 visual cortex spanning through presumptive areas 17 and 18. By using low levels of transfection, we ensured that change in gene expression was induced in isolated cells that were maintained in an intact environment (Figures 6A–6C). Specifically,

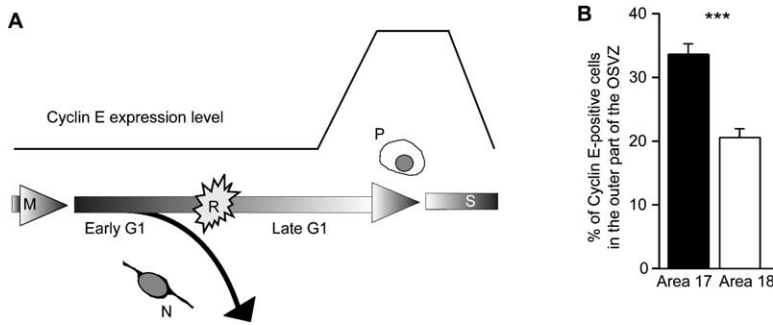


Figure 5. Frequency of Cell Cycle Reentry
(A) Cartoon showing how cyclin E informs on frequency of cell cycle reentry. The G1 phase is divided into early and late G1 separated by the restriction point (R). The restriction point corresponds to the time point where a cell is irreversibly committed to a new cycle. Molecules expressed after the restriction point distinguish between daughter cells that reenter the cycle and those that exit the cycle. Cyclin E expression characterizes late G1 and is therefore only expressed by daughter cells that reenter the cell cycle. Hence, changes in proportions of precursors that express cyclin E reflect variations in proportions of cells reentering the cell cycle.

(B) In vivo percentage of cyclin E-positive precursors in area 17 and area 18 OSVZ with respect to the total population of precursors. Values are \pm SEM. Statistical analysis with Mann-Whitney U test; *** $p < 0.0005$.

we asked whether up- or downmodulation of these two cell cycle regulators is able to alter the two cardinal parameters of cell cycle kinetics that are area-specifically regulated: Tc and frequency of cell cycle reentry. Downregulation of cyclin E and p27^{Kip1} was implemented on organotypic slices of E80 visual cortex by means of RNAi technique. siRNA were colipofected with the EGFP expression plasmid, so as to monitor cell cycle modifications of identified precursors (Figures 6A–6C). Some lipofected precursors showed a radial glial-like morphology with extended radial process, suggesting that, as in the mouse, a fraction of cortical precursors in the primate could be radial glial cells (Malatesta et al., 2000; Noctor et al., 2001) (Figures 6A–6C). We first checked that siRNA transfection resulted in a significant decrease of p27^{Kip1} and cyclin E expression. Confocal microscopy quantification of the immunolabeling against p27^{Kip1} in p27-siRNA-EGFP-colipofected cells performed after 3 DIV indicate a 33% decrease ($p < 0.001$) in expression levels compared to EGFP singly lipofected cells. Using an identical procedure, we found that cyclin E protein level expression was reduced by 28% ($p < 0.001$) in cyclin E-siRNA-EGFP-colipofected cells compared to EGFP singly lipofected cells. Forced expression of p27^{Kip1} and cyclin E was obtained via co-transfection of p27^{Kip1} and cyclin E expression plasmids with the EGFP expression plasmid, respectively. Transfection resulted in an expression increase of 55% for p27^{Kip1} and 100% for cyclin E as revealed by confocal quantification of immunolabeling.

Analysis of the influence of p27^{Kip1} downmodulation in cortical OSVZ precursors shows a significant increase in the proportion of Ki67-positive cells within the germinal zone, indicating an increase in cell cycle reentry (see Experimental Procedures) (22.6% increase; $p < 0.001$ using χ^2 test with Yate's correction; Figure 6D), while p27^{Kip1} forced expression results in a significant decrease of cell cycle reentry (19.8% decrease; $p < 0.001$; Figure 6D). In contrast, cyclin E downmodulation results in a decrease of cell cycle reentry as shown by lower percentages of Ki67-positive cells in the colipofected population compared to the EGFP singly lipofected cells (29.1% decrease; $p < 0.001$; Figure 6D), whereas cyclin E forced expression leads to a significant increase in the frequency of cell cycle reentry (14% increase; $p < 0.001$; Figure 6D).

In a second step, we investigated the influence of

p27^{Kip1} and cyclin E down- and upregulation on the rate of cell cycle progression. LI analysis in colipofected dissociated precursors reveals that both p27^{Kip1} forced expression and cyclin E downmodulation results in significantly decreased LI values, suggesting a lengthening of Tc, whereas p27^{Kip1} downmodulation and cyclin E forced expression lead to an increase in LI values, suggesting a shorter Tc, possibly via a reduced G1 phase (Lukaszewicz et al., 2002; Lukaszewicz et al., 2001) (Figure 6E). These results indicate that the p27^{Kip1} and cyclin E expression levels are at least partly responsible for regulating Tc in areas 17 and 18 primate cortical precursors.

By implementing low levels of transfection in E80 occipital cortical precursors, we have been able to show that p27^{Kip1} and cyclin E expression levels contribute to variations of cell cycle parameters that are observed in vivo in supragranular precursors of areas 17 and 18. We now need to address the significance of these results with respect to early areal specification. This requires implementing a large-scale population change in cell cycle regulators to examine whether, for instance, area 17 precursors can be induced to show cell cycle parameters comparable to that of area 18 precursors. This approach is possible using adenoviral-mediated gene transfer that allows a nearly 100% rate of infection (Craig et al., 1997; Lukaszewicz et al., 2001). Human p27^{Kip1} was overexpressed in area 17 precursors in E80 dissociated cultures, leading to an increase of 42% in the level of p27^{Kip1} expression. Compared with area 18 precursors, precursors of area 17 overexpressing p27^{Kip1} exhibit lower LI values (Figure 6G), pointing to a lengthening of Tc within the cycling population. Area 17 dissociated cell cultures overexpressing p27^{Kip1} also show diminished values of the fraction of PCNA-positive cells (GF) with respect to the total population (Figure 6H), indicating an increase in the fraction of precursors withdrawing from the cell cycle and therefore corresponding to a decrease in cell cycle reentry. As a consequence of the decrease in both LI and GF values, area 17 precursors overexpressing p27^{Kip1} are characterized by lower rates of proliferation as indicated by decreased CD (Figure 6I). Therefore, the present results show that p27^{Kip1} ectopic expression in area 17 precursors induces altered cell cycle characteristics. Under these conditions, area 17 precursors show lower rates of proliferation than area 18 precursors, indicating the involvement

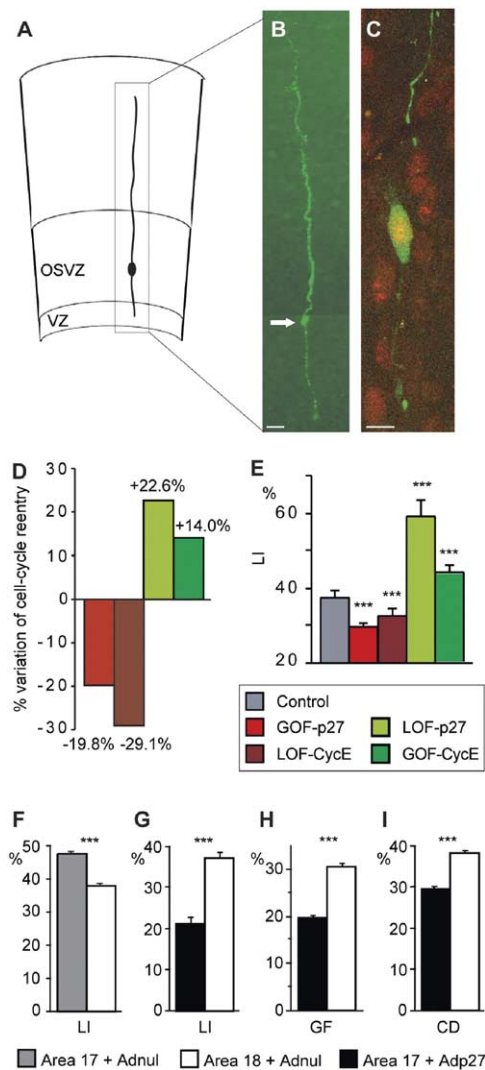


Figure 6. Analysis of Cell Cycle Parameters in p27^{Kip1} and Cyclin E Loss- and Gain-of-Function Experiments

(A) Drawing showing a lipofected precursor in an organotypic slice. (B) Microphotograph showing the GFP-lipofected precursor from (A) in the OSVZ. (C) Microphotograph of a Ki67-positive, GFP-lipofected precursor. (D) Histograms showing the percentage variation of the growth fraction (fraction of Ki67-positive cells in the germinal zones) indicating variation of cell cycle reentry value on organotypic slices. Control values correspond to precursors colipofected with control (pHPCAG) and EGFP plasmid or precursors colipofected with a nonsense control siRNA and EGFP plasmid. (E) Histograms showing LI values on dissociated cultures. Statistical significance was assessed with a χ^2 test. (F) LI variations in area 17 and area 18 OSVZ precursors infected with Adnl. Results showing variations of LI (G), GF (H), and CD (cell density [I]) in area 17 precursors overexpressing p27^{Kip1} via adenoviral infection compared to area 18 precursors infected by empty virus. Scale bars, 50 μ m in (B); 10 μ m in (C). For abbreviations, see Figure 2. Values are \pm SEM.

of p27^{Kip1} in regulating area-specific parameters of cortical proliferation.

These results provide evidence that p27^{Kip1} and cyclin E expression levels play a key role in regulating both cell cycle reentry and Tc. The present experimental up- and downmodulation of cyclin E and p27^{Kip1} show that, as in vivo in area 17 and area 18 of the primate (see

above) and as demonstrated in vitro in mouse cortical precursors (Lukaszewicz et al., 2002), both parameters are regulated in a coordinated fashion: short Tg1 is associated with a higher frequency of cell cycle reentry, whereas long Tg1 is correlated with lower frequencies of cell cycle reentry.

Modeling of Cell Cycle Parameters

So as to understand how regulation of Tc and frequency of cell cycle reentry can influence both the dimensions of the precursor pool and rates of neuron production, we have implemented modeling of cell cycle parameters using a compartmental mathematical model of cortical neurogenesis (Polleux et al., 1997).

Using the cell cycle parameters from the present report, we simulated corticogenesis spanning E70 to E85 to explore if experimentally observed areal differences in frequency of cell cycle reentry and Tc can account for both the increase in neuron production and the amplification of the precursor pool of area 17 compared to area 18 (Smart et al., 2002). At E70, precursor pools are identical in both areas. Between E70 and E85, there is an amplification of the precursor pool and an upsurge in neuron production, which are more pronounced in area 17 compared to area 18 (Smart et al., 2002). To obtain the correct approximation of the number of cycles in the 15 day period, we used Tc values of 36 hr (area 17) and 46 hr (area 18) (cf. results). We implemented differences in the cell cycle reentry of areas 17 and 18 obtained from cyclin E LI values after correcting for areal differences in Tc.

Implementing a shorter Tc in model area 17 precursors while maintaining an identical frequency of cell cycle reentry in both sets of precursors leads to only a modest increase in the rate of neuron production in area 17 relative to area 18. Further, under these conditions there is a failure to amplify the precursor pool in area 17 relative to area 18 (Figure 7A). Modeling shows that increased frequency of cell cycle reentry does in fact lead to increases and not decreases in rates of neuron production. This can be seen by implementing the calculated 20% higher rate of cell cycle reentry in model area 17 precursors while maintaining identical Tc values in both sets of precursors. This leads to a relatively larger amplification of the precursor pool of area 17 compared to area 18 as well as to an increase in the relative rate of neuron production in area 17. However, the 75% increase in rate of production of neurons in area 17 (Figure 7B) is inferior to the experimentally observed values that correspond to a 2- to 2.5-fold increase in the number of supragranular neurons in area 17 compared to area 18 (Rockel et al., 1980) (C.D. and H.K., unpublished data). It turns out that it is necessary to combine both the higher rates of cell cycle reentry and the shorter Tc values as observed in the present study in model area 17 precursors in order to obtain the increase in the rates of neuron production that are comparable to those observed in area 17 (Figure 7C).

Discussion

Primate-Specific Features of Cortical Neurogenesis

The SVZ undergoes an evolutionary expansion and is a major germinal zone in the monkey, where it is estab-

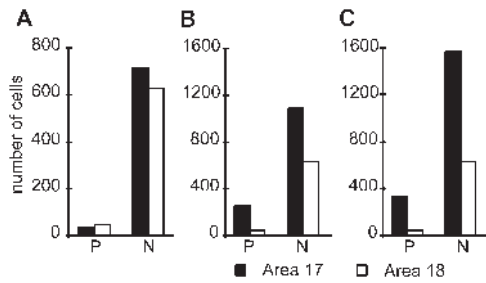


Figure 7. Mathematical Modeling Showing the Evolution of the Size of the Precursor Pool and Total Number of Postmitotic Neurons Produced during the 15 Day Simulation Period

Initial number of precursors (P) is identical in each case and arbitrarily fixed at 100 (see text). The simulation uses *in vivo* Tc values obtained in this study (A17, 36 hr; A18, 46 hr). (A) Here, the frequency of cell cycle reentry is made identical for areas 17 and 18. This simulation shows that cell cycle duration differences alone generate only a 14% difference in the number of neurons produced (N). (B) Here, Tc is fixed at 46 hr in both sets of precursors. Frequency of cell cycle reentry is set 20% higher in area 17 compared to area 18 (calculated from data of Figure 5 and corrected for variations in Tc). The simulation shows that cell cycle reentry difference alone generates a 75% difference in the number of neurons produced. (C) This simulation combines the experimentally observed 22% difference in cell cycle duration (36 versus 46 hr) and the observed 20% difference in cell cycle reentry (after correction for Tc). This generates a 151% difference in the number of neurons produced.

lished at the onset of neuron production at E55 (Smart et al., 2002). The OSVZ from E72 to the end of neuron production at E100 (Rakic, 1974) constitutes the major site of neuron production, in terms of both size and numbers of mitotically active cells (present work). This contrasts with the SVZ in mouse, which is not apparent before E13, and although it increases in volume up to the end of corticogenesis, it fails to acquire the importance observed in the monkey (Kostovic and Rakic, 1990; Smart et al., 2002; Smart and McSherry, 1982).

The present study showing that the OSVZ is the major site of the supragranular layer neuron production in the monkey agrees with findings showing common specific gene expression in both the SVZ and the supragranular neurons in rodents (Nieto et al., 2004; Tarabykin et al., 2001; Zimmer et al., 2004) as well as recent studies showing neurogenic production in the rodent SVZ (Haubensak et al., 2004; Noctor et al., 2004).

Tc of cortical precursors is considerably extended in primates (Kornack and Rakic, 1998). It has been suggested that the prolonged Tc in monkey cortical precursors is an adaptive feature related to the evolutionary expansion of neocortex in primates (Rakic, 1995). Because environmental signals are known to determine cortical precursor fate (McConnell and Kaznowski, 1991; Polleux et al., 2001) during the cell cycle as well as regulate rates of proliferation (Dehay et al., 2001), the prolonged primate Tc may serve to ensure a fine adjustment of the rates of production of phenotypically defined neurons.

Contribution of Cell Cycle Regulation and Frequency of Cell Cycle Reentry in Early Cortical Patterning

The results show that germinal zones of presumptive areas 17 and 18 are characterized by differences in

control of the cell cycle, indicating early mechanisms of areal specification. The *in vivo* quantification of cell cycle kinetics demonstrates the existence of areal differences in Tc via an area-specific control of Tg1. Kornack and Rakic reported combined variations in Ts and Tg1 phase duration in the VZ during corticogenesis of the rhesus monkey (Kornack and Rakic, 1998). This contrasts with the mouse, where Tg1 is considered to be the only regulated phase during corticogenesis (Caviness et al., 2003). Our measurements of Tc in the OSVZ fail to show areal variations in Ts and demonstrate that Tg1 variation accounts for the areal differences in Tc. Interestingly, this area-specific decrease in Tg1 occurs specifically during the amplification of the supragranular precursors pool (Smart et al., 2002). There is evidence pointing to G1 phase of the cell cycle being a window of increased sensitivity to differentiation signals (Mummary et al., 1987). It is thus tempting to speculate that shortening of G1 phase might shield area 17 cortical precursors from signals that induce cell cycle exit and differentiation.

The present *in vivo* observations provide evidence for an area-specific regulation of the frequency of cell cycle reentry during corticogenesis. Together with the observations of the G1 phase duration, the present results show an area-specific regulation of Tg1 associated with regulation of the balance between cell cycle exit and cell cycle reentry.

Conclusion and Perspectives

The areal differences in levels of expression of p27^{Kip1} and cyclin E combined with the single cell and tissue level up- and downmodulation experiments converge to indicate that levels of expression of these two G1/S transition regulators could contribute to area-specific differences in cell cycle kinetics. Mathematical modeling of areal differences in cell cycle parameters shows that alone they could account for the differences in neuron number that characterize these two areas. These results point to the essential role of cell cycle regulation in the early regional patterning of the cortex, at the level of the germinal zones (Piao et al., 2004; Rakic, 1988; Rakic, 2004).

The present results showing an area-specific cross-coordination of G1 phase duration and frequency of cell cycle reentry provide additional evidence for the link between G1 phase duration and frequency of cell cycle reentry that are regulated in a concerted fashion in mouse cortical progenitors (Lukaszewicz et al., 2002; Lukaszewicz et al., 2001).

It remains to be determined whether these areal differences in cell cycle regulation are intrinsic to the developing germinal zones, where they could constitute a readout of regionalized gene expression (Grove and Fukuchi-Shimogori, 2003; Monuki and Walsh, 2001; O'Leary and Nakagawa, 2002; Rakic, 1988). Areal cell cycle differences could also be the consequence of environmental factors acting on a protomap (Job and Tan, 2003; Kennedy and Dehay, 1993; Rakic, 1988; Sur and Leamey, 2001). Thalamic afferents, which have been shown to shorten Tg1 and increase cell cycle reentry (Dehay et al., 2001), could therefore fulfill this role in area 17.

Whatever the upstream control of area-specific corti-

cogenesis is, a central problem that remains is how the proliferative gradient in the germinal zone generating areas 17 and 18 is transcribed into a stepwise function at the 17/18 border in terms of differences in numbers of neurons (Kennedy and Dehay, 1993; Kennedy and Dehay, 2001). The morphogenetic events that are involved in the formation of the sharp border will involve differential rates of migration (H. Kennedy et al., 1996, Soc. Neurosci., abstract), proliferation (Dehay et al., 1993) (this report), and tangential expansion (Smart et al., 2002). While we do not know the molecular mechanisms integrating these diverse phenomena, they form part of an intriguing challenge in cortical development, since at no time during corticogenesis are sharply bordered patterns of genes observed in the germinal zones. Even genes differentially expressed in the early cortical plate show graded patterns, although at later stages of development many acquire an expression pattern with abrupt changes that correlate with borders between areas (Rubenstein et al., 1999; Sestan et al., 2001), as pointed out in a review by Nagakawa and O'Leary (O'Leary and Nakagawa, 2002).

Experimental Procedures

In Vivo Studies

Cynomolgus monkey fetuses of known gestational dates received approximately 10–20 $\mu\text{Ci/g.b.w.}$ (i.p. or i.m.) or 2 mCi (intraamniotically) of 3H-thymidine in saline (specific activity, 40–60 $\mu\text{Ci/mmol}$) and were replaced in the uterus according to previously described protocols (Dehay et al., 1993). Following caesarian section, anaesthetized fetuses were perfused through the heart with 4% paraformaldehyde (PFA). All experiments were performed in compliance with the national and European laws as well as with institutional guidelines concerning animal experimentation.

Observations in fetuses aged E64 and E78 were made prior to the appearance of a clear cytoarchitectonic border of striate cortex, and transient expression of acetylcholine esterase (Kostovic and Rakic, 1984) was used to infer the area 17/18 boundary (Smart et al., 2002). Brains used for 3H-thymidine studies were embedded in paraffin wax, and 5 or 10 μm thick parasagittal sections were cut. An E80 fetus was transcardially perfused with saline (0.9%) followed by 4% PFA in 0.1 M phosphate buffer and an increasing sucrose gradient (10%–20%) for cryoprotection. Sections (60 μm thick) were cut on a freezing microtome and were used for p27^{Kip1} and cyclin E immunocytochemistry.

In Vivo Cell Cycle Kinetics Measurements

3H-thymidine cumulative labeling (Nowakowski et al., 1989) makes it possible to derive the duration of S and G1 + G2/M phases. Two cumulative 3H-thymidine labeling experiments were performed at E78, during the generation of supragranular neurons. 3H-thymidine was administered intraamniotically via ultrasound-guided injection using a 22G needle. In one experiment, cumulative labeling was performed during 14 hr by means of eight injections (each injection consisted of a constant dose of 2 mCi) every 120 min. The successive injections spaced 2 hr apart (Kornack and Rakic, 1998) cumulatively labeled precursors that entered S phase during the 14 hr period. In the second experiment, two injections of 3H-thymidine were made (2 mCi) with the same time interval (120 min), corresponding to a 3 hr period exposure to 3H-thymidine.

One hour following the last injection, the fetuses were removed by caesarian section, lethally anaesthetized with sodium pentobarbital, and transcardially perfused with a mixture of PFA (4%) in PB.

The LI values were determined as the proportion of 3H-thymidine-positive cells (i.e., cells that were in S phase during the 3H-thymidine exposure) with respect to the OSVZ precursor population. In order to get accurate measurements, we have corrected those LI values so as to take into account the value of the GF. GF in the OSVZ of area 17 and area 18 was measured on 40 μm thick frozen sections from a -20°C ethanol-fixed E78 embryonic brain,

using PCNA as a marker of cycling cells. Computing percentage of PCNA-positive cells with respect to the total number of precursors using confocal microscopy examination reveals GF values of 88.9% and 90.2% for area 17 and area 18, respectively. As in the Kornack and Rakic (1998) study, we assumed that 3H-thymidine accumulation to saturation in the monkey OSVZ is linear, as demonstrated in rodents (Takahashi et al., 1995). In this context, it is appropriate to estimate Tc and Ts from a linear slope best fit to data from two survival times (3 hr and 14 hr).

PLM labeling (Quastler and Sherman, 1959) was used to determine G2/M duration. Two fetuses aged E78 received a pulse injection of 3H-thymidine (1.5 mCi) and were perfused, respectively, 2 and 7 hr following the pulse.

Statistical Analysis

For the PLM experiments, statistical significance was tested by means of a F test applied to the ascending slope of the curve. For 3H-thymidine cumulative labeling, statistical significance was tested by means of a generalized linear model using a binomial family (equivalent to a logistic regression) in which the covariates were time and visual area (McCullagh and Nelder, 1989). The statistical difference between areas was tested by means of a χ^2 test. All tests were performed in the R statistical computing environment (R Development Core Team, 2004). While only two points in time were sampled, four measurements were made at each time point and for both conditions. This makes it possible to model the data. In fact, there is not a single overlap in the sample distributions. Logistic regression shows that the visual area of origin generates a significantly different temporal evolution in the proliferation rate (χ^2 : 41.128; $p = 1.223 \times 10^{-10}$).

Dissociated Cell Culture

Fetal brains at E62, E78, and E80 were removed under sterile conditions in iced Hank's balanced salt solution containing 10 mM HEPES. Area 17 cells were obtained from the most caudal part of the occipital lobe, and presumptive area 18 cells were obtained from a more rostral location, on the posterior bank of the presumptive lunate sulcus. Cells were seeded and cultured as described elsewhere (Dehay et al., 2001).

Organotypic Slice Culture

Slices (200 μm thick) were cut through the occipital lobe (E80) spanning area 17 and area 18 with a Leica vibratome in 4°C HBSS. Slices were maintained in GMEM + 10% FCS on poly-L-lysine-laminin-coated transwells (Falcon Cell Culture Inserts, 1.0 μm pore size, 6-well format).

In Vitro Immunocytochemistry

PCNA/BrdU Double Labeling

Following fixation (ethanol 70%, -20°C), immunostaining was performed as described elsewhere (Dehay et al., 2001). Cells in S phase at the time of the exposure were positively stained for BrdU. Cycling precursors were identified by means of PCNA labeling. Nuclei were counterstained with Hoechst.

GFP/Ki67 Double Labeling

Following PFA fixation, slices and dissociated cells were processed as follows. Briefly, coverslips were rinsed three times in TBS-T 0.5%. Following incubation in normal goat serum (1:5 for 20 min) and the anti-Ki67 (mouse monoclonal Ab, clone NCL-Ki67-MM1, Novocastra; 1:100) and anti-GFP (Alexa Fluor 488 conjugate, Molecular Probes; 1:1000) were incubated in TBS overnight at 4°C. After three rinses, goat anti-mouse Cy3 (1:200 in Dako diluent; Jackson ImmunoResearch) was incubated for 1 hr at room temperature (RT). Coverslips were mounted with 0.1% n-propylgallate (P3130; Sigma) in a 1 M phosphate buffer and glycerol (1:1) to prevent fading on fluorescent illumination (Lukaszewicz et al., 2002).

GFP/BrdU Double Labeling

Slices and dissociated cells were fixed with PFA. BrdU immunostaining was performed as described elsewhere (Dehay et al., 2001). In addition, anti-GFP (Alexa Fluor 488 conjugate, Molecular Probes; 1:1000) was incubated in TBS overnight at 4°C. Coverslips were mounted as described above.

p27^{Kip1} Immunocytochemistry

After PCNA immunocytochemistry, coverslips were processed for p27^{Kip1} immunocytochemistry. Briefly, primary antibody incubation (rabbit anti-p27^{Kip1} from Santa Cruz Biotechnology, SC-528) was incubated at 1:20 in Dako diluent at RT for 1 hr. After three rinses, goat anti-rabbit Cy2 (1:200 in Dako diluent; Jackson ImmunoResearch) was incubated for 1 hr at RT. Coverslips were mounted as described above.

MAP2 Immunocytochemistry

MAP2 immunocytochemistry was performed as described elsewhere (Dehay et al., 2001).

Coverslips were examined using oil objective (×50 or ×100) under UV light to detect FITC (filter 450–490 nm) and Hoechst (filter 355–25 nm). Coverslips were scanned at regular intervals with a grid corresponding to a field of 0.128 mm². One hundred to one hundred and fifty fields were observed per coverslip. A minimum of two coverslips was observed for each condition. All experiments were done at least in duplicate.

Fluorescent labeling on organotypic slices was analyzed using a Leica confocal microscope, using a ×40 objective (see below for details).

In Situ Immunolabeling

Immunolabeling was performed according to a two-step procedure. Briefly, sections were incubated overnight at 4°C with primary antibodies p27^{Kip1} (Santa Cruz, SC-528; 1:200) and cyclin E (Santa Cruz, SC-481; 1:200). Sections were further incubated for 3 hr at RT with goat anti-rabbit-Cy3 (Interchim, 1:400 in DAKO diluent). Sections were counterstained with Syto16.

Anti-H3 immunocytochemistry was used to visualize mitotic figures in the OSVZ at E78 on frozen sections from PFA-fixed tissue. Briefly, rabbit anti-H3 (Upstate, 07-145) was incubated at 4°C overnight in TBS-T, followed by incubation of goat anti-rabbit Cy2 1/1000 in TBS-T at RT for 1 hr.

Real-Time PCR

Real-time PCR was performed on E82 microdissected germinal zones of area 17 and area 18 using the LightCycler Fast Start DNA Master SYBR Green I kit and a LightCycler (Roche). Primers for detection of cyclin E and β-actin were as follows. Cyclin E: cDNA length, 133 bp; annealing temperature, 64°C; 5' primer (5' to 3'), AGC ACT TCA GGG GCG TCG C; 3' primer (5' to 3'), CTG GGG AGA GGA GAA GCC C. β-actin: cDNA length, 101 bp; annealing temperature, 60°C; 5' primer (5' to 3'), GCG TGA TGG TGG GCA TGG; 3' primer (5' to 3'), GAT GCC GTG CAC GAT GGG.

Confocal Measurements of Cyclin E and p27^{Kip1} Expression Levels

We have quantified protein expression levels by means of confocal microscopy analysis (Durand et al., 1997; Lukaszewicz et al., 2002; Tokumoto et al., 2002). Confocal examination of the fluorescent labeling was carried out on a LEICA TCS SP equipped with an argon-krypton laser. Analysis of p27^{Kip1} and cyclin E expression was performed using an ×40 (40 μm brain sections) or an ×63 (dissociated cells) oil objective. Quantitative analysis of Cy2 and Cy3 fluorescence was performed using Leica software (TCS NT). The tissue expression levels in the germinal zone were determined by calculating the intensity of fluorescence (arbitrary units) of p27^{Kip1} or cyclin E labeling with respect to the total number of cells (indicated either by the intensity of Syto16 fluorescence or by cell counts) (Figure 4). Several fields of view were analyzed so as to span the entire thickness of the OSVZ, in area 17 and area 18. Levels of cyclin E immunofluorescence intensity have been measured for each cell expressing detectable levels of cyclin E. Four categories of labeling intensity have been defined: <50 (negative), 50–80 (low-intensity labeling), 80–110 (intermediate-intensity labeling), and >110 (high-intensity labeling). The LI of cyclin E-positive cells is determined by the percentage of cells showing detectable immunofluorescent intensity (>50) with respect to the total population of precursors (Figure 4). Confocal quantitative analysis of p27^{Kip1} immunofluorescence in PCNA-positive cell nuclei was performed on dissociated cell cultures. Statistical significance between area 17 and area 18 values was assessed with a Mann-Whitney U test.

Plasmid Constructs

Full-length cDNAs encoding mouse p27^{Kip1} (Toyoshima and Hunter, 1994) and mouse cyclin E (Dulic et al., 1992) were inserted into the unique BstXI site of the pNPCAG expression plasmid (Niwa et al., 1998) to generate pNPCAG-mp27 and pNPCAG-cycE, respectively.

siRNA Duplex

The siRNAs were purchased from Ambion, and the sequences were as follows: GGAAUAAGGAAGCGACCGTT (sense) and CAGGCG CUUCCUUAUUCCTG (antisense) predesigned siRNA p27, and GGAAAAGACAUCUUAAGGTT (sense) and CCUUAAGUAUGUCU UUUCCCTT (antisense) for *Silencer Validated* siRNA cyclin E1. The *Silencer Validated* siRNAs from Ambion are single siRNA duplexes that have been verified experimentally to reduce the expression of their individual target genes. Each siRNA has been shown and is guaranteed to reduce target gene expression by at least 70% 48 hr posttransfection via electroporation in human HeLa cells. The extent of mRNA knockdown elicited was compared to cells transfected with a nonsense control siRNA: the Silencer Negative Control #1 from Ambion (Ref 4611).

Lipofection

Constructs were lipofected using Lipofectamine 2000 (Invitrogen) according to the manufacturer's instructions with minor modifications. An EGFP reporter plasmid was colipofected to mark transfected cells. Colipofection efficiency has been estimated to be 85%–100% (Ohnuma et al., 2002). Briefly, transfection was carried out 24 hr following dissociated cell seeding or organotypic slice culture. After 1 day of incubation, the medium was changed. Slices and dissociated cultures were fixed and processed for cell cycle parameters 48 and 96 hr following lipofection. All experiments were done in triplicate.

Adenoviral Infection

Dissociated neuroblasts from a E80 brain were plated as described above. Fifteen hours later, a dose of 5 moi Adp27, coding for the human form of p27^{Kip1} (hp27^{Kip1}) (Craig et al., 1997), was added to the culture medium. The proliferation rates were assayed 48 hr after infection. Control cultures were infected with Adnul (an empty virus) (Craig et al., 1997).

Supplemental Data

The Supplemental Data include one figure and can be found with this article online at <http://www.neuron.org/cgi/content/full/47/3/353/DC1/>.

Acknowledgments

We are grateful to Dr. P. Seth for the gift of Adp27 and Adnul and to Dr. Iain Smart for spirited discussions. We thank Béatrice Morailon-de Rette for help with the mathematical modeling using MatLab and Ken Knoblauch for the statistical analysis. We are indebted to Delphine Autran for excellent technical assistance, to Florence Wianny and Nathalie Doerflinger for expertise and help with the siRNA experiments, and to Catherine Rey (Neurobiotec Service, IFR19) for assistance with the real-time PCR analysis. This work is supported by EU grant Concorde QLG3-2000-00158, Ministère de la Recherche; ACI 2002 Biologie du Développement et Physiologie Intégrative grant n°0220582; ACI 2003 Neurosciences Intégratives et Computationnelles grant n° 03568; and Fondation pour la Recherche Médicale FRM grant n°SOU20031114083.

Received: April 8, 2004

Revised: May 4, 2005

Accepted: June 28, 2005

Published: August 3, 2005

References

Baek, S.H., Kiuoussi, C., Briata, P., Wang, D., Nguyen, H.D., Ohgi, K.A., Glass, C.K., Wynshaw-Boris, A., Rose, D.W., and Rosenfeld, M.G. (2003). Regulated subset of G1 growth-control genes in re-

- sponse to derepression by the Wnt pathway. *Proc. Natl. Acad. Sci. USA* 100, 3245–3250.
- Bartek, J., and Lukas, J. (2001). Pathways governing G1/S transition and their response to DNA damage. *FEBS Lett.* 490, 117–122.
- Beaulieu, C., and Colonnier, M. (1989). The number of neurons in individual laminae of areas 3B, 4B and 6a alpha of the cat cerebral cortex: a comparison with major visual areas. *J. Comp. Neurol.* 279, 228–234.
- Caviness, V.S., Jr., Goto, T., Tarui, T., Takahashi, T., Bhide, P.G., and Nowakowski, R.S. (2003). Cell output, cell cycle duration and neuronal specification: a model of integrated mechanisms of the neocortical proliferative process. *Cereb. Cortex* 13, 592–598.
- Craig, C., Wersto, R., Kim, M., Ohri, E., Li, Z., Katayose, D., Lee, S.J., Trepel, J., Cowan, K., and Seth, P. (1997). A recombinant adenovirus expressing p27^{Kip1} induces cell cycle arrest and loss of cyclin-Cdk activity in human breast cancer cells. *Oncogene* 14, 2283–2289.
- Dehay, C., Giroud, P., Berland, M., Smart, I., and Kennedy, H. (1993). Modulation of the cell cycle contributes to the parcellation of the primate visual cortex. *Nature* 366, 464–466.
- Dehay, C., Savatier, P., Cortay, V., and Kennedy, H. (2001). Cell-cycle kinetics of neocortical precursors are influenced by embryonic thalamic axons. *J. Neurosci.* 21, 201–214.
- Dulic, V., Lees, E., and Reed, S.I. (1992). Association of human cyclin E with a periodic G1-S phase protein kinase. *Science* 257, 1958–1961.
- Durand, B., Gao, F.B., and Raff, M. (1997). Accumulation of the cyclin-dependent kinase inhibitor p27/Kip1 and the timing of oligodendrocyte differentiation. *EMBO J.* 16, 306–317.
- Ekholm, S.V., Zickert, P., Reed, S.I., and Zetterberg, A. (2001). Accumulation of cyclin E is not a prerequisite for passage through the restriction point. *Mol. Cell. Biol.* 21, 3256–3265.
- Garey, L.J., Winkelmann, E., and Brauer, K. (1985). Golgi and Nissl studies of the visual cortex of the bottlenose dolphin. *J. Comp. Neurol.* 240, 305–321.
- Grove, E.A., and Fukuchi-Shimogori, T. (2003). Generating the cerebral cortical area map. *Annu. Rev. Neurosci.* 26, 355–380.
- Haubensak, W., Attardo, A., Denk, W., and Huttner, W.B. (2004). Neurons arise in the basal neuroepithelium of the early mammalian telencephalon: a major site of neurogenesis. *Proc. Natl. Acad. Sci. USA* 101, 3196–3201.
- Job, C., and Tan, S.S. (2003). Constructing the mammalian neocortex: the role of intrinsic factors. *Dev. Biol.* 257, 221–232.
- Kennedy, H., and Dehay, C. (1993). Cortical specification of mice and men. *Cereb. Cortex* 3, 27–35.
- Kennedy, H., and Dehay, C. (2001). Gradients and boundaries: limits of modularity and its influence on the isocortex. *Dev. Sci.* 4, 147–148.
- Kioussi, C., Briata, P., Baek, S.H., Rose, D.W., Hamblet, N.S., Herman, T., Ohgi, K.A., Lin, C., Gleiberman, A., Wang, J., et al. (2002). Identification of a Wnt/Dvl/ β -Catenin \rightarrow Pitx2 pathway mediating cell-type-specific proliferation during development. *Cell* 111, 673–685.
- Kiyokawa, H., Kineman, R.D., Manova-Todorova, K.O., Soares, V.C., Hoffman, E.S., Ono, M., Khanam, D., Hayday, A.C., Frohman, L.A., and Koff, A. (1996). Enhanced growth of mice lacking the cyclin-dependent kinase inhibitor function of p27(Kip1). *Cell* 85, 721–732.
- Kornack, D.R., and Rakic, P. (1998). Changes in cell-cycle kinetics during the development and evolution of primate neocortex. *Proc. Natl. Acad. Sci. USA* 95, 1242–1246.
- Kostovic, I., and Rakic, P. (1984). Development of prefrontal visual projections in the monkey and human fetal cerebrum revealed by transient cholinesterase staining. *J. Neurosci.* 4, 25–42.
- Kostovic, I., and Rakic, P. (1990). Developmental history of the transient subplate zone in the visual cortex of the macaque monkey and human brain. *J. Comp. Neurol.* 297, 441–470.
- Letinic, K., Zoncu, R., and Rakic, P. (2002). Origin of GABAergic neurons in the human neocortex. *Nature* 417, 645–649.
- Lukaszewicz, A., Savatier, P., Cortay, V., Seth, P., Kennedy, H., and Dehay, C. (2001). G1 phase regulation and differentiation of mouse cortical precursors. Paper presented at: Stem and progenitor cells: Biology and applications (Cold Spring Harbor, New York).
- Lukaszewicz, A., Savatier, P., Cortay, V., Kennedy, H., and Dehay, C. (2002). Contrasting effects of bFGF and NT3 on cell cycle kinetics of mouse cortical stem cells. *J. Neurosci.* 22, 6610–6622.
- Malatesta, P., Hartfuss, E., and Gotz, M. (2000). Isolation of radial glial cells by fluorescent-activated cell sorting reveals a neuronal lineage. *Development* 127, 5253–5263.
- McConnell, S.K., and Kaznowski, C.E. (1991). Cell cycle dependence of laminar determination in developing neocortex. *Science* 254, 282–285.
- McCullagh, P., and Nelder, J.A. (1989). *Generalized Linear Models*, Second Edition (Boca Raton, FL: Chapman & Hall/CRC).
- Meyer, G., Schaaps, J.P., Moreau, L., and Goffinet, A.M. (2000). Embryonic and early fetal development of the human neocortex. *J. Neurosci.* 20, 1858–1868.
- Mitsuhashi, T., Aoki, Y., Eksioglu, Y.Z., Takahashi, T., Bhide, P.G., Reeves, S.A., and Caviness, V.S., Jr. (2001). Overexpression of p27Kip1 lengthens the G1 phase in a mouse model that targets inducible gene expression to central nervous system progenitor cells. *Proc. Natl. Acad. Sci. USA* 98, 6435–6440.
- Monuki, E.S., and Walsh, C.A. (2001). Mechanisms of cerebral cortical patterning in mice and humans. *Nat. Neurosci. Suppl.* 4, 1199–1206.
- Mummery, C.L., van den Brink, C.E., and de Laat, S.W. (1987). Commitment to differentiation induced by retinoic acid in P19 embryonal carcinoma cells is cell cycle dependent. *Dev. Biol.* 121, 10–19.
- Nakayama, K.I., Hatakeyama, S., and Nakayama, K. (2001). Regulation of the cell cycle at the G1-S transition by proteolysis of cyclin E and p27Kip1. *Biochem. Biophys. Res. Commun.* 282, 853–860.
- Nieto, M., Monuki, E.S., Tang, H., Imitola, J., Haubst, N., Khoury, S.J., Cunningham, J., Gotz, M., and Walsh, C.A. (2004). Expression of Cux-1 and Cux-2 in the subventricular zone and upper layers II–IV of the cerebral cortex. *J. Comp. Neurol.* 479, 168–180.
- Niwa, H., Burdon, T., Chambers, I., and Smith, A. (1998). Self-renewal of pluripotent embryonic stem cells is mediated via activation of STAT3. *Genes Dev.* 12, 2048–2060.
- Noctor, S.C., Flint, A.C., Weissman, T.A., Dammerman, R.S., and Kriegstein, A.R. (2001). Neurons derived from radial glial cells establish radial units in neocortex. *Nature* 409, 714–720.
- Noctor, S.C., Martinez-Cerdeno, V., Ivic, L., and Kriegstein, A.R. (2004). Cortical neurons arise in symmetric and asymmetric division zones and migrate through specific phases. *Nat. Neurosci.* 7, 136–144.
- Nowakowski, R.S., Lewin, S.B., and Miller, M.W. (1989). Bromodeoxyuridine immunohistochemical determination of the lengths of the cell cycle and the DNA-synthetic phase for an anatomically defined population. *J. Neurocytol.* 18, 311–318.
- Ohnuma, S., and Harris, W.A. (2003). Neurogenesis and the cell cycle. *Neuron* 40, 199–208.
- Ohnuma, S., Philpott, A., and Harris, W.A. (2001). Cell cycle and cell fate in the nervous system. *Curr. Opin. Neurobiol.* 11, 66–73.
- Ohnuma, S., Mann, F., Boy, S., Perron, M., and Harris, W.A. (2002). Lipofection strategy for the study of Xenopus retinal development. *Methods* 28, 411–419.
- O’Leary, D.D., and Nakagawa, Y. (2002). Patterning centers, regulatory genes and extrinsic mechanisms controlling arealization of the neocortex. *Curr. Opin. Neurobiol.* 12, 14–25.
- Oliver, T.G., Grasfeder, L.L., Carroll, A.L., Kaiser, C., Gillingham, C.L., Lin, S.M., Wickramasinghe, R., Scott, M.P., and Wechsler-Reya, R.J. (2003). Transcriptional profiling of the Sonic hedgehog response: a critical role for N-myc in proliferation of neuronal precursors. *Proc. Natl. Acad. Sci. USA* 100, 7331–7336.
- Piao, X., Hill, R.S., Bodell, A., Chang, B.S., Basel-Vanagaite, L., Straussberg, R., Dobyns, W.B., Qasrawi, B., Winter, R.M., Innes, A.M., et al. (2004). G protein-coupled receptor-dependent development of human frontal cortex. *Science* 303, 2033–2036.

- Polleux, F., Dehay, C., Morailon, B., and Kennedy, H. (1997). Regulation of neuroblast cell-cycle kinetics plays a crucial role in the generation of unique features of neocortical areas. *J. Neurosci.* *17*, 7763–7783.
- Polleux, F., Dehay, C., Goffinet, A., and Kennedy, H. (2001). Pre- and post-mitotic events contribute to the progressive acquisition of area-specific connectional fate in the neocortex. *Cereb. Cortex* *11*, 1027–1039.
- Polyak, K., Kato, J., Solomon, M.J., Sherr, C.J., Massague, J., Roberts, J.M., and Koff, A. (1994). P27kip1, a cyclin-Cdk inhibitor, links transforming growth factor- β and contact inhibition to cell cycle arrest. *Genes Dev.* *8*, 9–22.
- Quastler, H., and Sherman, F.G. (1959). Cell population kinetics in the intestinal epithelium of the mouse. *Exp. Cell Res.* *17*, 420–438.
- R Development Core Team (2004). R: A language and environment for statistical computing. (Vienna: R Foundation for Statistical Computing, ISBN 3-900051-07-0), <http://www.R-project.org>.
- Rakic, P. (1973). Kinetics of proliferation and latency between final division and onset of differentiation of cerebellar stellate and basket neurons. *J. Comp. Neurol.* *147*, 523–546.
- Rakic, P. (1974). Neurons in rhesus monkey visual cortex: systematic relation between time of origin and eventual disposition. *Science* *183*, 425–427.
- Rakic, P. (1988). Specification of cerebral cortical areas. *Science* *241*, 170–176.
- Rakic, P. (1995). A small step for the cell, a giant leap for mankind: a hypothesis of neocortical expansion during evolution. *Trends Neurosci.* *18*, 383–388.
- Rakic, P. (2004). Neuroscience. Genetic control of cortical convolutions. *Science* *303*, 1983–1984.
- Resnitzky, D., Gossen, M., Bujard, H., and Reed, S.I. (1994). Acceleration of the G1/S phase transition by expression of cyclin D1 and E with an inducible system. *Mol. Cell. Biol.* *14*, 1669–1697.
- Rockel, A.J., Hiorns, R.W., and Powell, T.P.S. (1980). The basic uniformity in structure of the neocortex. *Brain* *103*, 221–244.
- Rubenstein, J.L., Anderson, S., Shi, L., Miyashita-Lin, E., Bulfone, A., and Hevner, R. (1999). Genetic control of cortical regionalization and connectivity. *Cereb. Cortex* *9*, 524–532.
- Sestan, N., Rakic, P., and Donoghue, M.J. (2001). Independent parcellation of the embryonic visual cortex and thalamus revealed by combinatorial Eph/ephrin gene expression. *Curr. Biol.* *11*, 39–43.
- Sherr, C.J., and Roberts, J.M. (1999). CDK inhibitors: positive and negative regulators of G1-phase progression. *Genes Dev.* *13*, 1501–1512.
- Skoglund, T.S., Pasher, R., and Berthold, C.H. (1996). Heterogeneity in the columnar number of neurons in different neocortical areas in the rat. *Neurosci. Lett.* *208*, 97–100.
- Smart, I.H.M., and McSherry, G.M. (1982). Growth patterns in the lateral wall of the mouse telencephalon: II. Histological changes during and subsequent to the period of isocortical neuron production. *J. Anat.* *134*, 415–442.
- Smart, I.H.M., Dehay, C., Giroud, P., Berland, M., and Kennedy, H. (2002). Unique morphological features of the proliferative zones and postmitotic compartments of the neural epithelium giving rise to striate and extrastriate cortex in the monkey. *Cereb. Cortex* *12*, 37–53.
- Sur, M., and Leamey, C.A. (2001). Development and plasticity of cortical areas and networks. *Nat. Rev. Neurosci.* *2*, 251–262.
- Takahashi, T., Nowakowski, R.S., and Caviness, V.S. (1995). The cell cycle of the pseudostratified ventricular epithelium of the embryonic murine cerebral wall. *J. Neurosci.* *15*, 6046–6057.
- Tarabykin, V., Stoykova, A., Usman, N., and Gruss, P. (2001). Cortical upper layer neurons derive from the subventricular zone as indicated by Svet1 gene expression. *Development* *128*, 1983–1993.
- Tokumoto, Y.M., Apperly, J.A., Gao, F.B., and Raff, M.C. (2002). Posttranscriptional regulation of p18 and p27 Cdk inhibitor proteins and the timing of oligodendrocyte differentiation. *Dev. Biol.* *245*, 224–234.
- Toyoshima, H., and Hunter, T. (1994). p27, a novel inhibitor of G1 cyclin-Cdk protein kinase activity, is related to p21. *Cell* *78*, 67–74.
- Wimmel, A., Lucibello, F.C., Sewing, A., Adolph, S., and Muller, R. (1994). Inducible acceleration of G1 progression through tetracycline-regulated expression of human cyclin E. *Oncogene* *9*, 995–997.
- Zetterberg, A., Larsson, O., and Wiman, K.G. (1995). What is the restriction point? *Curr. Opin. Cell Biol.* *7*, 835–842.
- Zimmer, C., Tiveron, M.C., Bodmer, R., and Cremer, H. (2004). Dynamics of Cux2 expression suggests that an early pool of SVZ precursors is fated to become upper cortical layer neurons. *Cereb. Cortex* *14*, 1408–1420.
- Zindy, F., Soares, H., Herzog, K.-H., Morgan, J., Sherr, C.J., and Roussel, M.F. (1997). Expression of INK4 inhibitors of cyclin D-dependent kinases during mouse brain development. *Cell Growth Differ.* *8*, 1139–1150.
- Zindy, F., Cunningham, J.J., Sherr, C.J., Jogal, S., Smeyne, R.J., and Roussel, M.F. (1999). Postnatal neuronal proliferation in mice lacking Ink4d and kip1 inhibitors of cyclin-dependent kinases. *Proc. Natl. Acad. Sci. USA* *96*, 13462–13467.